

TDDFT WITH SKYRME FORCES: EFFECT OF TIME-ODD DENSITIES ON ELECTRIC GIANT RESONANCES

V.O. Nesterenko¹, W. Kleinig^{1,2}, J. Kvasil³, P. Vesely³, and P.-G. Reinhard⁴

¹ *Bogoliubov Laboratory of Theoretical Physics,*

Joint Institute for Nuclear Research,

Dubna, Moscow region, 141980, Russia

² *Technische Univirsitat Dresden, Inst. für Analysis, D-01062, Dresden, Germany*

³ *Institute of Particle and Nuclear Physics,*

Charles University, CZ-18000 Praha 8, Czech Republic and

⁴*Institut für Theoretische Physik II,*

Universität Erlangen, D-91058, Erlangen, Germany

Abstract

Time-odd densities and their effect on electric giant resonances are investigated within the self-consistent separable random-phase-approximation (SRPA) model for various Skyrme forces (SkT6, SkO, SkM*, SIII, SGII, SLy4, SLy6, SkI3). Time-odd densities restore Galilean invariance of the Skyrme functional, violated by the effective-mass and spin-orbital terms. In even-even nuclei these densities do not contribute to the ground state but can affect the dynamics. As a particular case, we explore the role of the current density in description of isovector E1 and isoscalar E2 giant resonances in a chain of Nd spherical and deformed isotopes with A=134-158. Relation of the current to the effective masses and relevant parameters of the Skyrme functional is analyzed. It is shown that current contribution to E1 and E2 resonances is generally essential and fully determined by the values and signs of the isovector and isoscalar effective-mass parameters of the force. The contribution is the same for all the isotope chain, i.e. for both standard and exotic nuclei.

I. INTRODUCTION

Skyrme forces [1, 2] are widely used for exploration of the ground state and excitations in atomic nuclei. In particular, last years big effort was done in application of these forces to exotic nuclei, nuclear matter and astrophysical problems (for recent reviews see [3, 4]). However, in spite of the impressive progress, Skyrme forces still suffer some serious troubles. For example, there are too many Skyrme parametrizations and the forces do require a unification. Further, being successful in description of the nuclear ground states, Skyrme forces often fail in a comprehensive treatment of nuclear dynamics (e.g. no one force can describe equally well both isoscalar and isovector modes, see [5] for recent discussion). So, the further upgrade of the forces is necessary and nuclear dynamics should play here an important role.

In this connection, we propose here the analysis of time-odd densities in the Skyrme functional and their role in description of electric giant resonances (GR). Time-odd densities (current \vec{j} , spin \vec{s} , and vector kinetic-energy \vec{T}) are known to restore Galilean invariance of the Skyrme functional, violated by velocity-dependent time-even densities (kinetic-energy τ and spin-orbital $\vec{\mathfrak{S}}$) [6, 7]. Therefore time-odd densities are related to important features of the functional (effective masses and spin-orbital interaction) and might play an essential role in its upgrade. In this paper, we discuss time-odd densities in general and, as a particular case, scrutinize the influence of the current density \vec{j} on the isovector E1(T=1) and isoscalar E2(T=0) GR in a chain of Nd isotopes with A=134-158. As compared with the previous studies [5, 11], much more nuclei and forces are involved to make the exploration indeed systematic. We will establish important relations of the GR properties to specific parameters and terms of Skyrme forces and, on these grounds, propose a tentative classification of the forces.

The calculations are performed within the self-consistent random-phase-approximation (SRPA) method with factorized Skyrme forces [5, 8, 9, 10, 12]. SRPA covers both spherical [9] and deformed [5, 12] nuclei. Factorization minimizes the computational effort minimized and makes possible the systematic exploration.

II. TIME-ODD DENSITIES

A. General properties

The Skyrme functional [1] in the form [2, 6, 7, 13]

$$E = \int d\vec{r} (\mathcal{H}_{\text{kin}} + \mathcal{H}_{\text{C}}(\rho_p) + \mathcal{H}_{\text{pair}}(\chi_q) + \mathcal{H}_{\text{Sk}}(\rho_q, \tau_q, \vec{s}_q, \vec{j}_q, \vec{\mathfrak{S}}_q)) , \quad (1)$$

includes kinetic, Coulomb, pairing and Skyrme terms respectively. Expressions for the first three terms are done elsewhere [9, 11, 12, 13]. The Skyrme part reads

$$\begin{aligned} \mathcal{H}_{\text{Sk}} = & \frac{b_0}{2} \rho^2 - \frac{b'_0}{2} \sum_q \rho_q^2 - \frac{b_2}{2} \rho(\Delta\rho) + \frac{b'_2}{2} \sum_q \rho_q(\Delta\rho_q) \\ & + \frac{b_3}{3} \rho^{\alpha+2} - \frac{b'_3}{3} \rho^\alpha \sum_q \rho_q^2 + b_1(\rho\tau - \vec{j}^2) - b'_1 \sum_q (\rho_q \tau_q - \vec{j}_q^2) \\ & - b_4 \left(\rho(\vec{\nabla} \vec{\mathfrak{S}}) + \vec{s} \cdot (\vec{\nabla} \times \vec{j}) \right) - b'_4 \sum_q \left(\rho_q(\vec{\nabla} \vec{\mathfrak{S}}_q) + \vec{s}_q \cdot (\vec{\nabla} \times \vec{j}_q) \right) \\ & + \tilde{b}_4 \left(\vec{s} \vec{T} - \vec{\mathfrak{S}}^2 \right) + \tilde{b}'_4 \sum_q \left(\vec{s}_q \vec{T}_q - \vec{\mathfrak{S}}_q^2 \right) . \end{aligned} \quad (2)$$

This part involves time-even (nucleon ρ_q , kinetic-energy τ_q , and spin-orbital $\vec{\mathfrak{S}}_q$) and time-odd (current \vec{j}_q , spin \vec{s}_q , and vector kinetic-energy \vec{T}_q) densities, where q denotes protons and neutrons. The total densities (like $\vec{j} = \vec{j}_p + \vec{j}_n$) are given in (2) without the index.

Both time-even and time-odd densities follow from the original Skyrme forces [1]. Time-even densities contribute to both ground state and excitations. Time-odd densities affect the excitations as well. They also influence g.s. of odd and odd-odd nuclei but are irrelevant for g.s. of spin-saturated even-even nuclei.

As was mentioned above, time-odd densities restore Galilean invariance of the functional, violated by velocity-dependent time-even densities τ_q and $\vec{\mathfrak{S}}_q$ [6, 7]. Just for this reason, time-odd densities enter the functional only in the specific combinations with their time-even counterparts. Hence, time-odd densities do not lead to any new parameters. This is especially useful for even-even nuclei where Skyrme parameters, being fixed for the g.s. with implementation of the time-even densities only, can be further applied to nuclear dynamics involving time-odd densities as well.

Explicit expressions for time-even and time-odd densities via single-particle wave functions can be found elsewhere [3, 5, 7, 9, 13]. It is more instructive to write down these

densities in terms of the *basic* scalar ρ_q and vector \vec{s}_q densities

$$\rho_q(\vec{r}, \vec{r}') = \sum_{\sigma} \rho(\vec{r}\sigma, \vec{r}'\sigma'), \quad s_q^{\nu}(\vec{r}, \vec{r}') = \sum_{\sigma\sigma'} \rho_q(\vec{r}\sigma, \vec{r}'\sigma') \langle \sigma' | \hat{\sigma}_{\nu} | \sigma \rangle \quad (3)$$

which form a general one-body density matrix [6]

$$\rho_q(\vec{r}\sigma, \vec{r}'\sigma') = \frac{1}{2} [\rho_q(\vec{r}, \vec{r}') \delta_{\sigma, \sigma'} + \sum_{\nu} \langle \sigma | \hat{\sigma}_{\nu} | \sigma' \rangle s_q^{\nu}(\vec{r}, \vec{r}')] . \quad (4)$$

Here $\hat{\sigma}_{\nu}$ is a Pauli matrix and $\sigma = \pm 1$. Then the densities in (2) read as [6]

$$\rho_q(\vec{r}) = \rho_q(\vec{r}, \vec{r}), \quad \vec{s}_q(\vec{r}) = \vec{s}_q(\vec{r}, \vec{r}), \quad (5)$$

$$\vec{j}_q(\vec{r}) = \frac{1}{2i} [(\vec{\nabla} - \vec{\nabla}') \rho_q(\vec{r}, \vec{r}')]_{\vec{r}=\vec{r}'}, \quad \vec{\mathfrak{S}}_q^{\mu\nu}(\vec{r}) = \frac{1}{2i} [(\vec{\nabla}_{\mu} - \vec{\nabla}'_{\mu}) s_q^{\nu}(\vec{r}, \vec{r}')]_{\vec{r}=\vec{r}'}, \quad (6)$$

$$\tau_q(\vec{r}) = [\vec{\nabla} \cdot \vec{\nabla}' \rho_q(\vec{r}, \vec{r}')]_{\vec{r}=\vec{r}'}, \quad \vec{T}_q(\vec{r}) = [\vec{\nabla} \cdot \vec{\nabla}' \vec{s}_q(\vec{r}, \vec{r}')]_{\vec{r}=\vec{r}'}, \quad (7)$$

i.e. are reduced to the basic densities (5), their momenta (6) and kinetic energies (7). This presentation clarifies physical sense of the densities in terms of hydrodynamics. Besides, the presentation (5)-(7) can be treated as some kind of the gradient expansion up to the second derivatives of the basic densities. Such expansion is obviously useful for non-uniform densities, which is the case for \vec{s}_q and ρ_q at the nuclear boundary [3].

B. Current density

Between time-odd densities, the current is most important for electric GR. Indeed, the spin density \vec{s}_q is mainly relevant for magnetic modes and does not influence electric GR [5, 11]. The density \vec{T}_q can also be neglected as it supplements in (2) the term \mathfrak{S}_q^2 which is commonly omitted in most of the Skyrme forces.

Contribution of \vec{j}_q to the residual interaction is driven by the variation [5, 9]

$$\frac{\delta^2 E}{\delta \vec{j}_{q'}(\vec{r}') \delta \vec{j}_q(\vec{r})} = 2[-b_1 + b'_1 \delta_{q,q'}] \delta(\vec{r}' - \vec{r}) \quad (8)$$

which is fully determined by the terms $\sim b_1, b'_1$ in the functional (2). In these terms, the current density adjoins the values $\rho\tau$ and $\rho_q\tau_q$ responsible for the effective mass. Hence, one may expect the correlation between effective masses and \vec{j}_q in GR dynamics.

To inspect this correlation, it is convenient to express the terms $\sim b_1, b'_1$ through isoscalar and isovector densities $\rho_0 = \rho_n + \rho_p$ and $\rho_1 = \rho_n - \rho_p$ (the same for τ and \vec{j}). Then the sum

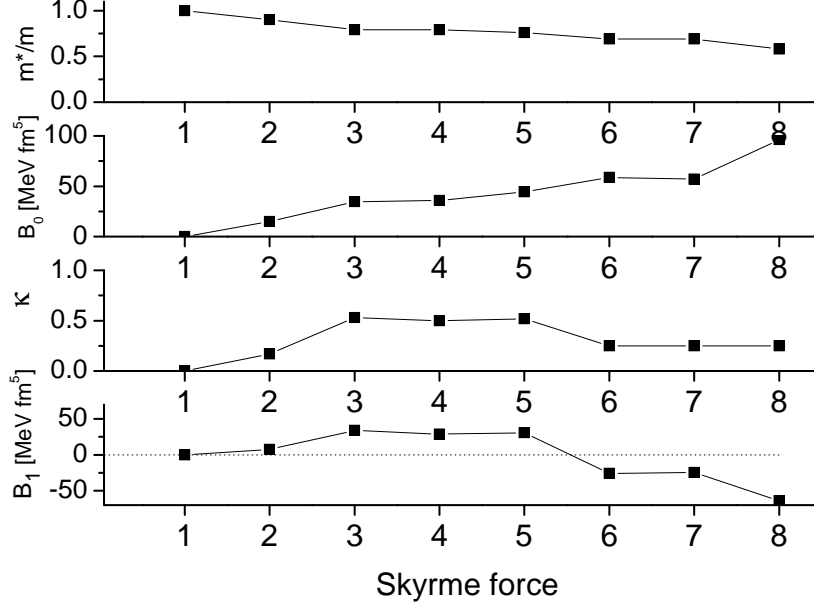


FIG. 1: Isoscalar B_0 and isovector B_1 force parameters as well as related isoscalar effective masses m^* and isovector enhancement factors κ for the Skyrme forces SkT6 (1), SkO (2), SkM* (3), SGII (4), SIII (5), SLy4 (6), SLy6 (7) and SkI3 (8). The dotted line at the bottom plot marks zero value.

of the terms with b_1 and b'_1 is transformed to the form

$$B_0(\rho_0\tau_0 - j_0^2) - B_1(\rho_1\tau_1 - j_1^2) \quad (9)$$

where isoscalar and isovector contributions are decoupled and $B_0 = b_1 - b'_1/2$ and $B_1 = b'_1/2$ [4]. For the symmetric nuclear matter, the isoscalar effective mass m^*/m and the sum-rule enhancement factor $\kappa = (m_1^*/m)^{-1} - 1$ (where m_1^*/m is the isovector effective mass) can be expressed via the new parameters as

$$\left(\frac{m^*}{m}\right)^{-1} = 1 + 2\frac{m}{\hbar^2}\bar{\rho}B_0, \quad \kappa = \frac{2m}{\hbar^2}\bar{\rho}(B_0 + B_1) \quad (10)$$

where m is the bare nucleon mass and $\bar{\rho}$ is the density of the symmetric nuclear matter. The relations (10) are illustrated in Fig. 1 for the set of Skyrme forces used in this paper. We see that there indeed take place correlations $B_0 \leftrightarrow m^*/m$ and $B_1 \leftrightarrow \kappa$. In the Section 4 we will show that \vec{j}_q -impact to E2(T=0) and E1(T=1) GR is also determined by the parameters B_0 and B_1 . This will justify the relation between \vec{j}_q and effective masses.

The velocity- and spin-dependent densities in the Skyrme functional should influence energy-weighted sum rules (EWSR) [14, 15]. For electric modes, contributions of spin-dependent densities $\vec{\mathcal{S}}$, \vec{s} and \vec{T} to EWSR can be neglected (though for Skyrme forces with

a low m^* , like SkI3, influence of the spin-orbital density $\vec{\mathfrak{S}}$ can be noticeable and reach 7-8% [16]). Instead the contributions of τ and \vec{j} are essential. The former alone results in the effective mass. However, for isoscalar modes the τ and \vec{j} contributions fully compensate each other [15]. So, if we take \vec{j} into account, then EWSR($T=0$) again acquires the bare mass m and becomes

$$EWSR(T = 0, \lambda > 1) = \frac{(\hbar e)^2}{8\pi m} \lambda(2\lambda + 1)^2 A < r^{2\lambda-2} >_A . \quad (11)$$

Such compensation is not complete for isovector modes [15] and EWSR($T=1, \lambda \geq 1$) retains the effective mass. In particular,

$$EWSR(T = 1, \lambda = 1) = \frac{(\hbar e)^2}{8\pi m_1^*} 9 \frac{NZ}{A} . \quad (12)$$

III. CALCULATION SCHEME

The study was performed with the representative set of 8 Skyrme forces: SkT6 [17], SkO [18], SIII [19], SGII [20], SkM* [21], SLy4 [22], SLy6 [22], SkI3 [23]. The isovector and isoscalar parameters and characteristics of these forces relevant for our study are exhibited in Fig. 1. We used the SRPA approach [5, 8, 9, 10, 12] in the approximation of 5 input operators of a different radial dependence. Four operators were chosen following prescription [9]. For deformed nuclei, the operator $r^{\lambda+2}Y_{\lambda+2,\mu}$ was added to take into account the multipole mixing of excitations with the same projection μ^π and parity π . Direct and exchange Coulomb contributions to the residual interaction were taken into account. As was shown in our previous studies [5, 9, 11], the proper choice of the input operators results in sensitivity of the separable residual interaction to both surface and interior dynamics. Hence high accuracy of the calculations was achieved already for a few separable terms. Factorization of the residual interaction results in drastic simplification of RPA calculations, which allows systematic calculations even for heavy spherical and deformed nuclei. It should be emphasized that factorization in SRPA is fully self-consistent and does not lead to additional parameters.

The giant resonances were computed as energy-weighted strength functions

$$S(E\lambda\mu; E) = \sum_{\nu} E_{\nu} M_{\lambda\mu\nu}^2 \zeta(E - E_{\nu}) \quad (13)$$

smoothed by the Lorentz function $\zeta(\omega - \omega_{\nu}) = \Delta / [2\pi((E - E_{\nu})^2 + (\Delta/2)^2)]$ with the averaging parameter Δ . In all the calculations $\Delta = 2$ Mev which was found to be optimal for the

comparison with experiment and simulation of various physical smoothing factors. Further, $M_{\lambda\mu\nu}$ is the matrix element of $E\lambda\mu$ transition from the ground state to the RPA state $|\nu\rangle$, E_ν is the RPA eigen-energy. We directly compute the strength function (13) and hence fully avoid determination of the numerous RPA eigen-states. This additionally reduces the computation time. SRPA calculations of GR in one nucleus at a familiar laptop take less than one hour, as compared with weeks while using full RPA methods [24].

The E1(T=1) and E2(T=0) resonances were computed with the proton and neutron effective charges $e_p^{eff} = N/A$, $e_n^{eff} = -Z/A$ and $e_p^{eff} = e_n^{eff} = 1$, respectively. A large configuration space was used. E.g. in ^{150}Nd we took into account 247 proton and 307 neutron single-particle levels ranging from the bottom of the potential well up to $\sim +20$ MeV. This results in 13000 and 22000 2-quasiparticle configurations for E1(T=1) and E2(T=0) excitations, respectively, with the energies up to 65 MeV. Then, EWSR (11) and (12) are exhausted by 93-99% and 95-97%, depending on the force.

IV. RESULTS AND DISCUSSION

Results of the SRPA calculations are presented in Figs. 2-7. In Figs. 2 and 3 the resonances E1(T=1) and E2(T=0) in ^{150}Nd are exhibited for eight Skyrme forces. It is seen that all the forces give in general acceptable agreement with the experiment for E1(T=1) resonance, which confirms ability of SRPA to describe isovector modes. For E2(T=0) we have no experimental data and so give the empirical estimation. It is seen that all the forces, for exception of SkT6 and SkO, overestimate the E2(T=0) energy and the lower the isoscalar effective mass m^* of the force, the more the overestimation. Figs. 2 and 3 demonstrate that no one force can describe simultaneously E1(T=1) and E2(T=0). This is especially the case for the forces with $m^*/m < 0.8$.

Figures 2 and 3 compare results obtained with and without \vec{j} -contribution to the residual interaction. The careful inspection of the figures shows that \vec{j} -contribution always improves description of E2(T=0) but not of E1(T=1). Moreover, the current always results in the down shift for E2(T=0) but may cause various shifts for E1(T=1). By comparing Figs. 2 and 3 with Fig. 1, one can see that \vec{j} -effects in E2(T=0) and E1(T=1) are fully determined by parameters B_0 and B_1 , respectively. The isoscalar parameter B_0 is positive for all the forces and steadily increases from SkT6 to SkI3. Hence we have for E2(T=0) the shift of

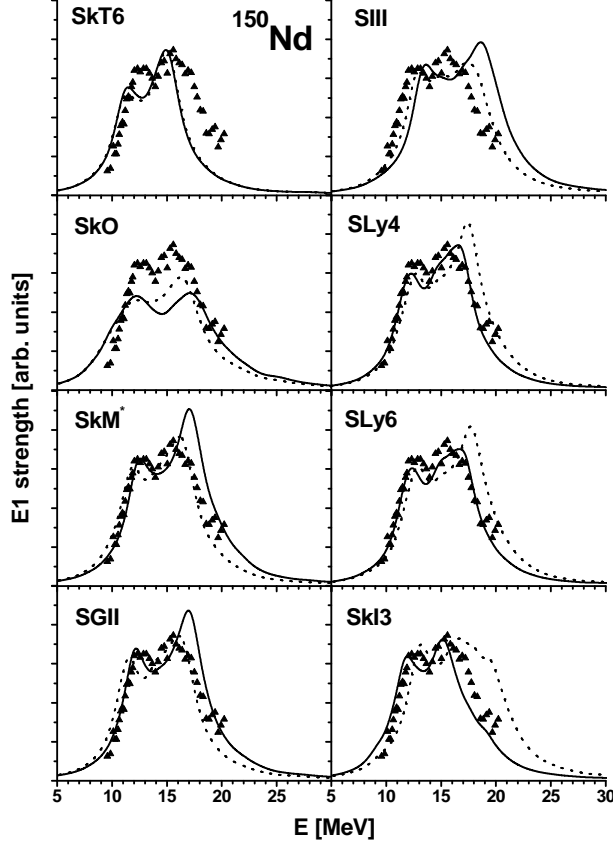


FIG. 2: $E1(T=1)$ giant resonance in ^{150}Nd , calculated with the Skyrme forces SkT6, SkO, SkM*, SGII, SIII, SLy4, SLy6 and SkI3 for the cases with (solid curve) and without (dotted curve) contribution of the time-odd current. The strength is smoothed by the Lorentz weight with the averaging $\Delta=2$ MeV. The experimental data [25, 26, 27] are depicted by triangles.

the same sign for all the forces and magnitude of the shift rises from SkT6 to SkI3. Instead, the isovector parameter B_1 is zero and small for SkT6 and SkO, positive for SGII, SIII and SkM* and negative for SkT4, SkT6 and SkI3. Hence we have negligible (SkT6), up (SkM*, SGII, SIII) or down (SkT4, SkT6, SkI3) shifts of $E1(T=1)$. Magnitude of the shifts obviously correlates with the absolute values of B_1 .

The above analysis allows to separate the Skyrme forces into 3 groups, depending on their B_0 and B_1 parameters. In the first group (SkT6, SkO) these parameters are zero or small, the effective masses are equal or close to the bare nucleon mass, and the role of the current density is negligible. These forces usually well describe $E2(T=0)$ but fail for $E1(T=1)$. The second group (SGII, SIII, SkM*) has larger B_0 and B_1 and therefore smaller effective masses. What is important, B_1 here is positive. These forces are usually fitted by GR

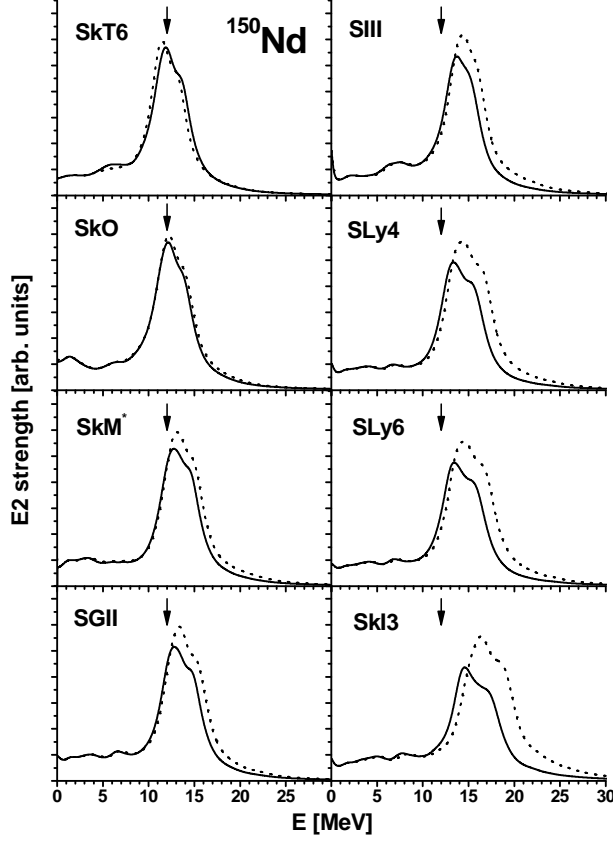


FIG. 3: The same as in Fig. 1 for E2(T=0) giant resonance. The empirical estimation for the resonance energy, $E = 62A^{-1/3}$ MeV, is marked the arrows.

as well (without taking into account time-odd densities). Hence they provide a reasonable description of GR. In this case, adding \vec{j} -contribution can even worsen the description, as we see in Fig. 2. These forces violate Galilean invariance and so can hardly be considered as a robust basis for the further upgrade. The third group of the forces (SLy4, Sly6, SkI3) is characterized by low effective masses and, what is important, by the negative value of B_1 . These forces (at least SLy4 and Sly6) well describe E1(T=1) but essentially overestimate the E2(T=0) energy. No one of the three groups is perfect. More systematic work with Skyrme forces is necessary.

Now we turn to systematic exploration of E1(T=1) resonance in the chain of Nd isotopes. The calculations were performed with the force SLy6 which, following Fig.2 and our previous studies [5, 11], promises one of the best descriptions of E1(T=1). Fig. 4 represents E1(T=1) in the isotopes where we have the photoabsorption experimental data. The isotopes run from the spherical semi-magic ^{142}Nd to the axially deformed ^{150}Nd discussed above. The $\mu = 0$

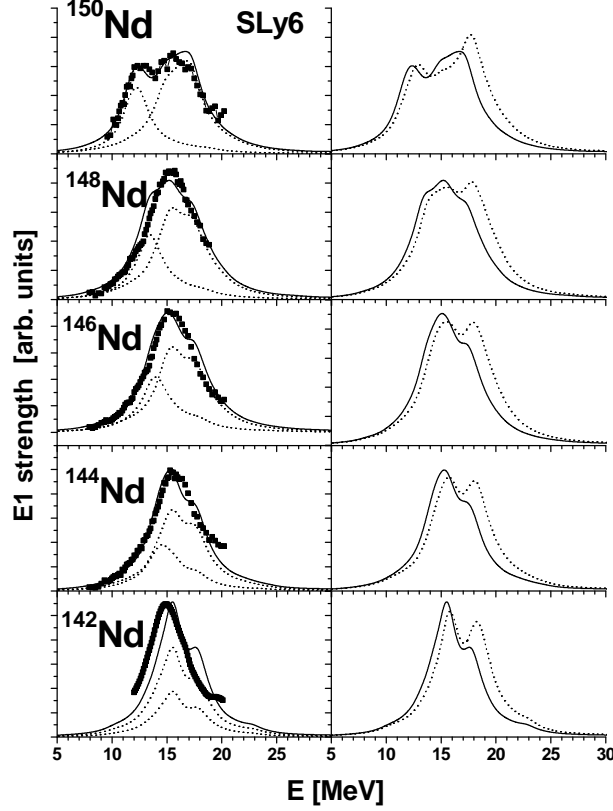


FIG. 4: The dipole giant resonance in Nd isotopes with $A=142-150$, calculated with the Skyrme forces SLy6. The left panels exhibit the full strength (solid curve) calculated with the current contribution. The $\mu = 0$ (left small peak) and $\mu = 1$ (right big peak) branches of the resonance are exhibited by dotted curves. The experimental data [25, 26, 27] are depicted by triangles. The right panels compare the full dipole strengths calculated with (solid curve) and without (dotted curve) current contribution.

and $\mu = 1$ brunches of the resonance are exhibited to illustrate the magnitude and kind (prolate) of the deformation. The figure demonstrates a remarkable agreement with the experiment for all the nuclei, maybe for exception of ^{142}Nd . Following right plots of the figure, the current contribution is the same for all the isotopes.

In Fig. 5, Nd isotopes with the neutron deficit ($A=134-140$) and excess (152-158) are explored. It is interesting that most of the isotopes are deformed and exhibit prolate shape. The cartesian quadrupole moments for the isotopes are given in Fig. 6. This figure also shows $E1(T=1)$ centroids and widths. The latter obviously correlate with the magnitude of the deformation. The resonance energies generally agree with estimation $E = 81A^{-1/3}$

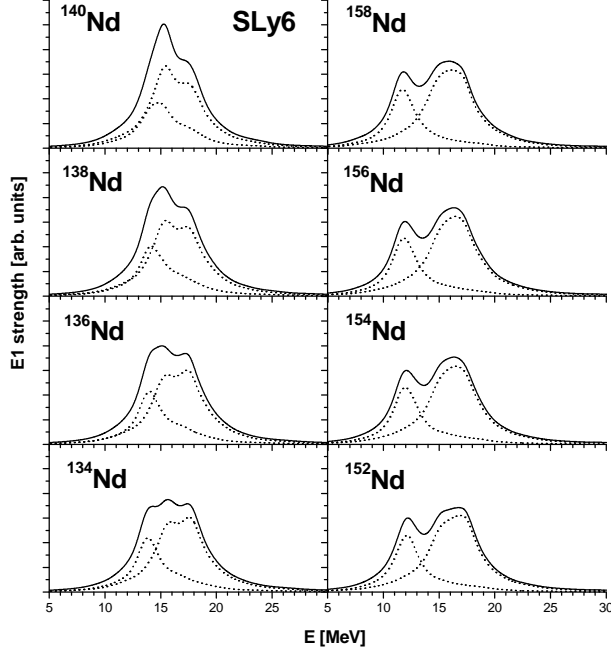


FIG. 5: The dipole giant resonance in Nd isotopes with $A=134-140$ and $152-158$, calculated for the force SLy6 with the current contribution. The full strength (solid curve) is supplemented by $\mu = 0$ and $\mu = 1$ branches (dotted curve).

MeV.

Finally, Fig. 7 demonstrates that the current density contribution to $E1(T=1)$ ends of the isotope chain is the same as in the middle of the chain (compare Figs. 4 and 7). So \vec{j} -impact is fully determined by the Skyrme force and does not depend on the shape and neutron number of the isotope. Since \vec{j} -impact is related with the effective masses, this observation sends a promising message that results for time-odd densities and effective masses obtained for standard nuclei may be relevant for exotic areas as well.

V. CONCLUSIONS

The effect of time-odd densities was discussed and examined for the particular case of the current density. The contribution of this density to $E1(T=1)$ and $E2(T=0)$ giant resonance was explored in the chain of Nd isotopes for a representative set of 8 Skyrme forces. The current impact was found to be generally strong and fully determined by the isoscalar and isovector parameters B_0 and B_1 of the Skyrme forces, responsible for the effective masses. The results obtained allow to classify the Skyrme forces into 3 groups, depending on the

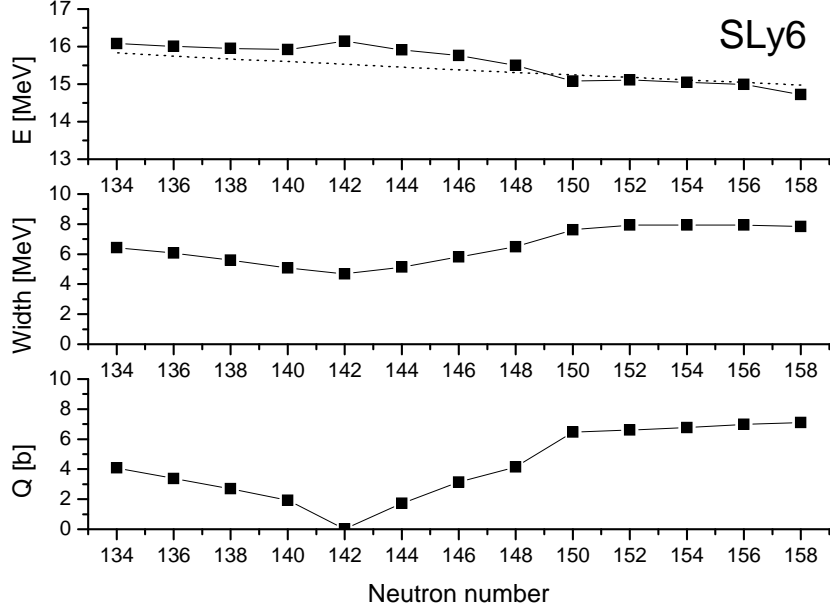


FIG. 6: Energies (upper plot) and widths (middle plot) of the dipole resonance, calculated (SLy6, with the current contribution) in Nd isotopes with $A=134-158$. The bottom plot exhibits the calculated quadrupole moments of the isotopes. Dotted line at the upper plot gives the empirical estimation $E = 81A^{-1/3}$ MeV for $E1(T=1)$ energy.

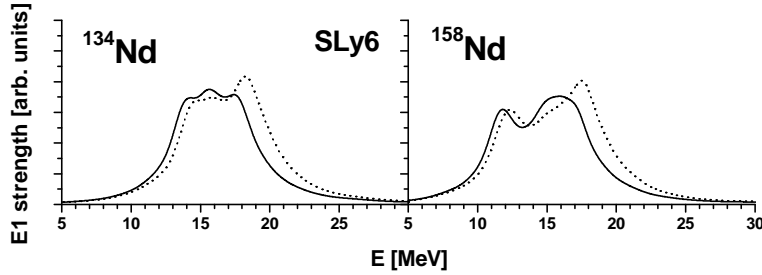


FIG. 7: The dipole resonance calculated with the force SLy6 for the cases with (solid curve) and without (dotted curve) contribution of the time-odd current in the isotopes ^{134}Nd and in ^{158}Nd .

magnitude and sign of B_1 . Our study show that time-odd densities represent a principle ingredient of Skyrme forces, responsible for the Galilean invariance. They are closely related with the effective masses and significantly influence nuclear dynamics. So, time-odd densities can be an important factor for further upgrade and unification of Skyrme forces.

The calculations show that the current impact is fully determined by the Skyrme force and does not depend on the shape or neutron number of the isotope. In other words, the impact is the same for standard and exotic nuclei. This message hints an interesting possibility to

explore the time-odd density effects for standard nuclei (where there are experimental data) and then to transfer the results to exotic areas.

Acknowledgments

The work was partly supported by DFG grant RE 322/11-1 and Heisenberg-Landau (Germany-BLTP JINR) grants for 2006 and 2007 years. W.K. and P.-G.R. are grateful for the BMBF support under contracts 06 DD 139D and 06 ER 808. This work is also a part of the research plan MSM 0021620834 supported by the Ministry of Education of the Czech Republic. It was partly funded by Czech grant agency (grant No. 202/06/0363) and grant agency of Charles University in Prague (grant No. 222/2006/B-FYZ/MFF).

-
- [1] T.H.R. Skyrme, *Phil. Mag.* **1**, 1043 (1956).
 - [2] D. Vauterin, D.M. Brink, *Phys. Rev.* **C5**, 626 (1972).
 - [3] M. Bender, P.-H. Heenen, and P.-G. Reinhard, *Rev. Mod. Rhys.* **75**, 121 (2003).
 - [4] J.R. Stone and P.-G. Reinhard, *Prog. Part. Nucl. Phys.* **58**, 587 (2007).
 - [5] V.O. Nesterenko, W. Kleinig, J. Kvasil, P.-G. Reinhard, and P. Vesely, *Phys. Rev. C* **74**, 054306 (2006).
 - [6] Y.M. Engel, D.M. Brink, K. Goeke, S.J. Krieger, and D. Vauterin, *Nucl. Phys.* **A249**, 215 (1975).
 - [7] J. Dobaczewski and J. Dudek, *Phys. Rev. C* **52**, 1827 (1995).
 - [8] J. Kvasil, V.O. Nesterenko, and P.-G. Reinhard, in *Proceed. of 7th Inter. Spring Seminar on Nuclear Physics*, Miori, Italy, 2001, edited by A.Covello, World Scient. Publ., p.437, 2002; ArXiv nucl-th/00109048.
 - [9] V.O. Nesterenko, J. Kvasil, and P.-G. Reinhard, *Phys. Rev. C* **66**, 044307 (2002).
 - [10] V.O. Nesterenko, J. Kvasil and P.-G. Reinhard, *Progress in Theoretical Chemistry and Physics* **15**, 127 (2006).
 - [11] V.O. Nesterenko, W. Kleinig, J. Kvasil, P. Vesely, and P.-G. Reinhard, *Int. J. Mod. Phys. E* **16**, 624 (2007).

- [12] V.O. Nesterenko, J. Kvasil, W. Kleinig, P.-G. Reinhard, and D.S. Dolci, ArXiv: nucl-th/0512045.
- [13] P.-G. Reinhard, Ann. Phys. (Leipzig) **1**, 632 (1992).
- [14] O. Bohigas, A.M. Lane, J. Martorell, Phys. Rep. **51**, 267 (1979).
- [15] E. Lipparini and S. Stringari, Phys. Rep. **175**, 103 (1989).
- [16] V.O. Nesterenko, W. Kleinig, J. Kvasil, P. Vesely, and P.-G. Reinhard, to be published in Proceed. of 26th Intern. Workshop on Nucl. Theory (Rila, Bulgaria, 2007).
- [17] F. Tondeur, M. Brack, M. Farine, and J.M. Pearson, Nucl. Phys. **A420**, 297 (1984).
- [18] P.-G. Reinhard, D.J. Dean, W. Nazarewicz, J. Dobaczewski, J.A. Maruhn, M.R. Strayer, Phys. Rev. C **60**, 14316 (1999).
- [19] M. Beiner, H. Flocard, Nguen Van Giai, and P. Quentin, Nucl. Phys. **A238**, 29 (1975).
- [20] N. Van Giai and H. Sagawa, Phys. Lett. **106B**, 379 (1981).
- [21] J. Bartel, P. Quentin, M. Brack, C. Guet, and H.-B. Håkansson, Nucl. Phys. **A386**, 79 (1982).
- [22] E. Chabanat, P. Bonche, P. Haensel, J. Meyer, and R. Schaeffer, Nucl. Phys. **A627**, 710 (1997).
- [23] P.-G. Reinhard and H. Flocard, Nucl. Phys. **A584**, 467 (1995).
- [24] J.A. Maruhn, P.-G. Reinhard, P.D. Stevenson, J. Rikovska Stone, and M.R. Strayer, Phys. Rev. C **71**, 064328 (2005).
- [25] P. Carlos, H. Beil, R. Bergere, A. Lepretre, and A. Veyssiere, Nucl. Phys. **A172**, 437 (1971).
- [26] B.L. Bergman and S.C. Fultz, Rev. Mod. Phys. **47**, 713 (1975).
- [27] A.V. Varlamov, V.V. Varlamov, D.S. Rudenko and M.E. Stepanov, Atlas of Giant Resonances, INDC(NDS)-394, 1999; JANIS database.